Published in *Proceedings of the 2023 International Conference on Clean Electrical Power (ICCEP)*, Terrasini, Italy, 27-29 june 2023, which should be cited to refer to this work.
DOI: 10.1109/ICCEP57914.2023.10247440

Dynamic Analysis of Future Scenarios of Power Systems Dominated by Inverter-Based Renewable Resources

G. Maione*, P. Morey**, M. Carpita**, M. Bozorg**, G. M. Tina*
*University of Catania, giovanni.maione@phd.unict.it, (Italy)
**HEIG-VD, mokhtar.bozorg@heig-vd.ch, (Switzerland)

Abstract—**Conventional power plants based on synchronous generators are being replaced with renewable energy sources, consequently increasing the proportion of inverter-based resources in the system. In this context, the total grid inertia is decreasing and system services that were traditionally delivered by synchronous generator need to be provided by inverter-based resources. To this end, it is necessary to develop and implement advanced inverter controls, such as grid-forming capability, that allow the provision of newly defined services. In this paper, dynamic analyses are performed, using DigSilent PowerFactory, on a power system with a significant presence of inverter-based resources. The study is based on the Swiss future scenarios. The effectiveness of grid forming inverters, based on droop control as well as virtual synchronous machine algorithms, on frequency support is studied. The results show that grid forming inverters have the potential to counteract the negative effects of traditional grid following inverter-based resources, as currently used by renewable power plants.**

Index Terms—**GFM inverter, frequency stability, RES integration.**

I. INTRODUCTION

A radical transformation of modern electrical power systems (EPSs) is needed to reduce greenhouse gas emissions and achieve sustainable objectives. This marks the transition from large centralized thermal power plants to smaller and distributed production units based on renewable energy sources (RESs), particularly wind turbines and photovoltaic (PV) plants. This transition requires increasing the percentage of electricity production from RESs through the installation of new capacity and the decommissioning of thermal units, including the complete phase-out of coal. Each European country has developed its own national strategy to meet the EU's targets. In this paper, Switzerland's future generation mix scenario, which is presented in PE2050+ [1], is considered. The Reference Scenario, based on the ZERO-base scenario, fixes objectives for the target years 2030 and 2040, with reference to 2019, see Table 1.

Generation from RESs is constrained by the stochastic nature of the primary energies exploited, e.g., wind speed and solar radiation intensity. The non-programmability of these resources poses a first challenge in the management of modern EPSs: system adequacy, under normal and emergency conditions. A second challenge arises from the technological nature of inverter-based RES systems, which is the stability of power systems. In effect, synchronous generators (SGs) have a physical inertia, linked to the grid frequency, that naturally provides support in the event of a transient. Whereas IBRs intrinsically have no inertia. As the proportion of IBRs to SGs increases, the total inertia of the EPS decreases, consequently leading to more severe transients. For this reason, grid forming (GFM) inverters with virtual inertia will play a critical role in the future.

Main paper contribution is the investigation on how GFM inverters can support the grid with a high presence of RESs, based on the Swiss expected future scenarios. In the following sections, GFM inverters will be tested as frequency support devices in a HV network. In particular, the ability to provide synthetic inertia and primary control will be evaluated.

TABLE I
FUTURE GENERATION MIX SCENARIOS FOR SWITZERLAND

	Installed capacity		
	2019	**CH2030**	**CH2040**
Hydroelectric	69.08%	58.18%	42.29%
Nuclear	14.99%	4.15%	0%
Thermoelectric	4.14%	3.37%	2.13%
Photovoltaics	11.34%	33.22%	52.85%
Wind	0.45%	1.05%	2.53%
Other RES	0%	0.03%	0.2%
Total	**22'220 MW**	**29'410 MW**	**45'540 MW**

II. INVERTER BASE RESOURCES CLASSIFICATION FOR PROVIDING ACTIVE POWER SERVICES.

Within the transition process of EPSs, IBRs represent both the cause of problems and possible solutions. While it is true that static converters create a separation between grid quantities and the energy source, it is also true that their great flexibility, due to their control modes, makes these devices indispensable for the future EPSs. All inverters are based on two control approaches: Grid following and grid forming [2][3]. The main differences between the two different control approaches are the following:

- **Grid Following (GFL):** the inverter is current controlled. It reads the grid voltage and injects current to provide the required active/reactive power. It keeps the current constant, even during transients, appearing to the grid as a constant current source. It stays synchronized to the grid with a phase-locked loop (PLL). If the PLL cannot accurately and quickly follow the external voltage, a GFL inverter cannot maintain a stable output current.
- **Grid Forming (GFM):** the inverter is voltage controlled. It creates its own voltage phasor based on the difference

between the actual active/reactive power and the required ones. The injected current is a consequence of the voltage that it imposes. It is capable of functioning on dominant and weak grids as well as in island mode. It maintains a constant internal voltage phasor, even during transients, appearing to the grid as a voltage source. This allows the GFM-IBRs to respond immediately to changes in the grid's voltage phasor providing support during a transient.

Unlike SGs that have an intrinsic physical behavior, IBRs' behavior is dictated by their control strategy. This allows IBRs be designed to provide different responses depending on the operational conditions. This control flexibility can be used to provide different ancillary services. For example, the following frequency services can be provided to enhance system stability [2][3]:

- **Synthetic inertia** emulates the inertial response of SGs. This service consists in active power injection proportional to the measured rate of change of frequency (RoCoF), starting a few milliseconds after the disturbance. This response is configurable.
- **Fast frequency response** is designed to support the grid in the event of frequency deviations and to counteract the effects of reduced inertia. It consists in fast active power injection proportional to the measured frequency deviation. The inverter's response is fast, configurable and can be done with or without frequency dead-band.

In the case of systems dominated by IBRs, these two services can make up for the lack of services provided by SGs. However, the provision of these new services is dependent on the control strategy of the inverter. Indeed, only GFM inverters can provide synthetic inertia services, because they can impose their voltage phasor on the grid, responding to the disturbance as it occurs. GFL inverters, on the other hand, are unable to provide this type of service because they follow the grid. GFL control can provide the fast frequency response service, emulating the governor of a SG, but with a faster response time. To maintain high stability requirements, it is necessary to integrate GFM-IBRs.

III. GFM INVERTER FOR GRID USAGE: STATE OF ART

As mentioned, inverters for grid applications are divided into GFL and GFM. Almost all the IBRs and RESs installed in the current EPSs are based on GFL control. This approach relies on the assumption that a sufficient number of SGs provide stable voltage and frequency ensuring a stiff grid. Unfortunately, as the number GFL-IBRs increases, the system is weakened, which increases the risk of instabilities.

New advanced controls, like GFM, are required to maintain system stability even in the case of extremely high IBR penetration. The GFM approach has been investigated since the 1990s, focusing on small power systems, e.g., microgrids or small islands. Examples are present in Kauai, Hawaii, rural areas in Alaska, and on university and military campuses [4][5].

Today, the implementation of GFM inverters is being considered in large EPSs due to their ability to improve stability. However, on the other hand, current research [4] has shown that stability issues in hybrid EPSs can occur due to interactions between the excitation system of SGs and IBRs. Nevertheless, mitigation methods are being developed to solve these issues.

Among the different GFM inverter control approaches, see [3][6], the most common are the Droop control and the Virtual Synchronous Machine (VSM) control. The main concepts of these two methods are:

- **Droop:** this control approach uses the droop equations (1), where there is a linear relationship between active power deviation, Δp, and frequency deviation, $\Delta\omega$, as well as between reactive power deviation, Δq, and voltage deviation, Δv. The constants, m_p and m_q, are the droop coefficients. This is used to control the voltage phasor of the inverter.

$$\Delta\omega = m_p\,\Delta p\ ;\ \Delta v = m_q\,\Delta q \tag{1}$$

- **VSM**: this control method emulates the behaviour of a SG by implementing the mathematical model of the swing equation (2). A common feature is the emulation of the mechanical inertia of SGs.

$$T_a\frac{d\omega}{dt} = D_p\,(\omega_{set} - \omega_r) + p_{set} - p_{mea} \tag{2}$$

Where T_a is the mechanical time constants representing the inertia, D_p is the damping coefficient, ω_{set} and p_{set} are the setpoint speed and power, ω_r and p_{mea} are the actual speed and power.

IV. SIMULATIONS

To assess the impact of IBRs and GFM converters on the EPS frequency transients, dynamic analyses are done running simulations in DigSilent PowerFactory.

Here, three scenarios are developed: the first called "Base scenario" is based on the IEEE 9 bus system, described in [7] (structure and load flow) which represents a network where all the generation is synchronous, as in the 2019 data in Table I (~90% SGs). The second and third scenarios, called "CH2030" and "CH2040", implement a substantial presence of RES generation as foreseen. Furthermore, two extra scenarios are done, based on the two previous ones, where the two GFM approaches (Droop and VSM) are added in support to the grid. These new scenarios are designated as "CH2030 GFM" and "CH2040 GFM".

A. Base scenario

The test network used in this scenario and the load flow results are shown in Fig.1. To carry out the dynamic analyses on this system, a 20% load variation is applied in 200ms at Load8 (at $t = 1s$) to evaluate the frequency transient behavior. The three generators represent hydroelectric (Gen1) and thermal units (Gen2, Gen3). The inertia constants are 9.55s, 3.92s and 2.77s, while the droop coefficients are 4% (Gen1) and 10% (Gen2, Gen3). The simulation results are shown in Fig. 2 and Fig. 3, where the frequency transient and the power profiles of the generators are displayed. The applied disturbance causes a frequency nadir of 49.669Hz, that is reached at $t = 5.47s$. During the first instants of the transient, the generators provide their inertial response to counteract the disturbance and mitigate the frequency deviation. Then, thanks to the action of the governors, the power of the generators settles to their steady-state value after about 50s at which point the frequency reaches 49.866Hz.

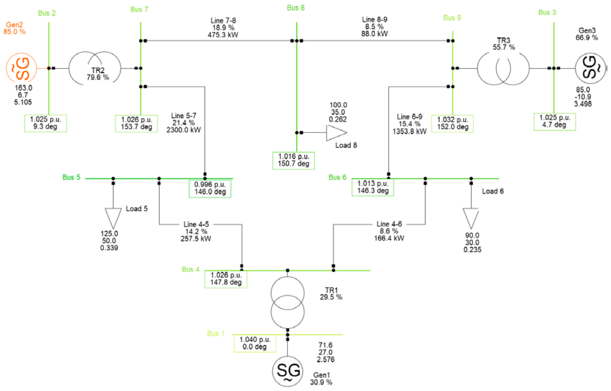

Fig. 1. Test network and load flow results, for the Base Scenario.

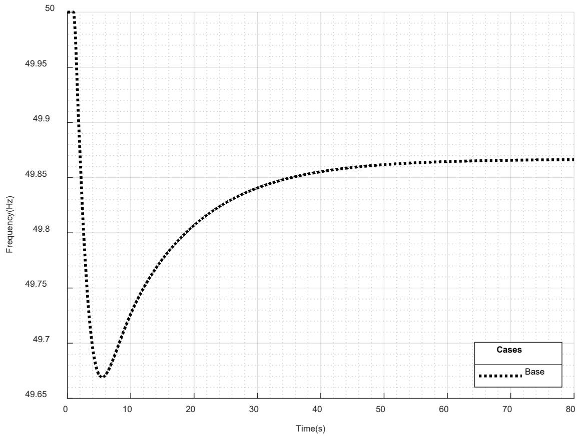

Fig. 2. Frequency response for the Base scenario

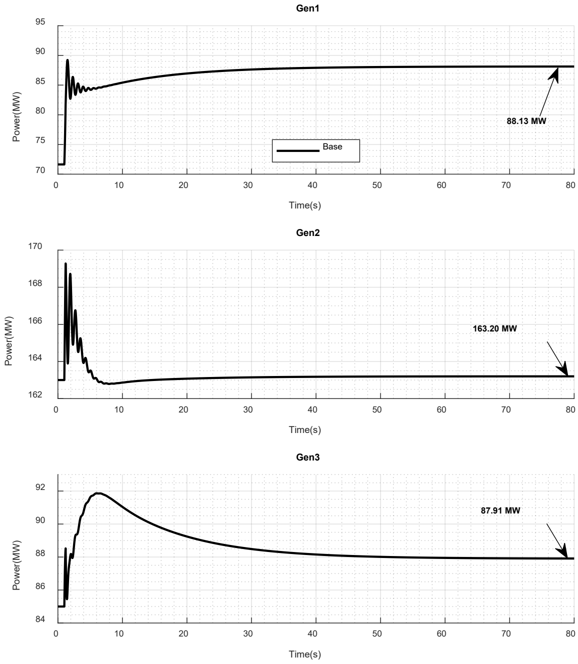

Fig. 3. Active power response for the Base scenario.

B. CH2030 Scenario

This near-future scenario has been made considering the Swiss expected installed capacity in 2030 (see Table 1). In this scenario, approximately 34% of the installed generation is RESs, of which practically all is PV. For the test grid to reflect this percentage, the synchronous thermal generation represented by Gen2 is replaced by an equivalent RES generator. This unit is implemented using the DER-A model, which can be seen as the aggregation of several PV generators [8]. The simulation results are reported in Fig. 4 and 5.

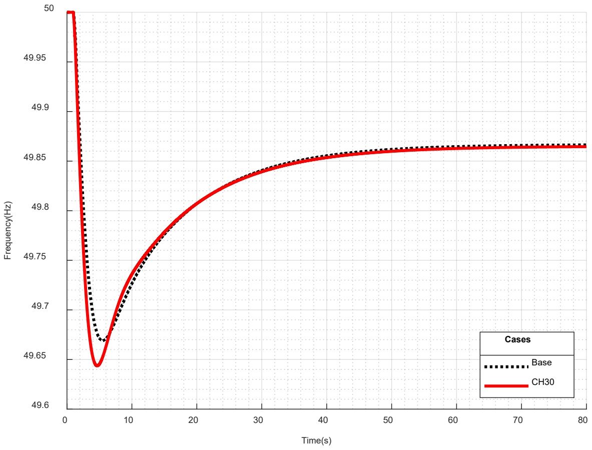

Fig. 4. Frequency response for the CH2030 scenario

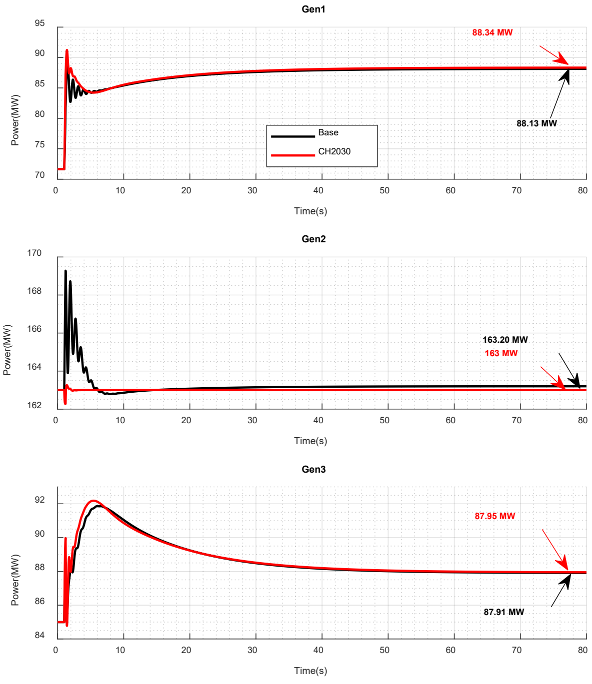

Fig. 5. Active power response for the CH2030 scenario.

As known, conventional PV generation does not contribute to the total system inertia. Furthermore, these units currently work in a way that maximizes the available energy, so they are unable to provide grid support during underfrequency events. Replacing synchronous generation with PV leads to a decrease in system inertia and regulating power. Fig. 4 compares the frequency transient between the Base and CH2030 scenario. It shows that with the same disturbance, the latter’s transient has a greater RoCoF that causes a lower nadir (49.644Hz) reached at $t = 4.60s$. The steady state frequency stabilizes 2 mHz lower at 49.864Hz. In this case the difference is small because the Gen2 is close to its maximum power, meaning that its substitution with PV has a small impact on the steady state frequency.

Analyzing Fig. 5 in contrast to the Base scenario, the presence of the equivalent PV generator, which does not participate in frequency regulation, causes the two other SGs to increase their active power output to contain the frequency deviation and stabilize the frequency.

C. CH2030 GFM Scenario

The aim of this scenario is to evaluate the effectiveness of GFM inverters in improving the frequency stability in the CH2030 scenario. To show the impact of GFM inverters, a modeled 10 MVA GFM device is added to bus 8 to support the network. The model can be seen as representative of many distributed GFM inverters. Two GFM models are tested, the first is with Droop control and the second is a VSM. These models are available in DigSilent’s library and are used with their default parameters. The frequency results obtained for these simulation cases are shown in Fig. 6, where the profiles of the various scenarios are compared. It can be observed that the presence of these devices significantly improves the frequency transient, especially in the first few seconds. Thanks to their ability to emulate SGs, these devices can provide active power in support of the frequency in a few milliseconds. They help the system to contain the frequency variation, resulting in a lower RoCoF and a higher nadir value. In the case of the Droop GFM Inverter, the frequency reaches a nadir of 49.730Hz at $t = 4.09s$, whereas for the VSM GFM Inverter, the nadir is reached at $t = 4.31s$ and has a value of 49.722Hz. Concerning the steady state frequency value, a clear improvement can be noticed using the Droop GFM Inverter. The steady state frequency is 49.880Hz and 49.865Hz respectively for the Droop and VSM GFM inverters.

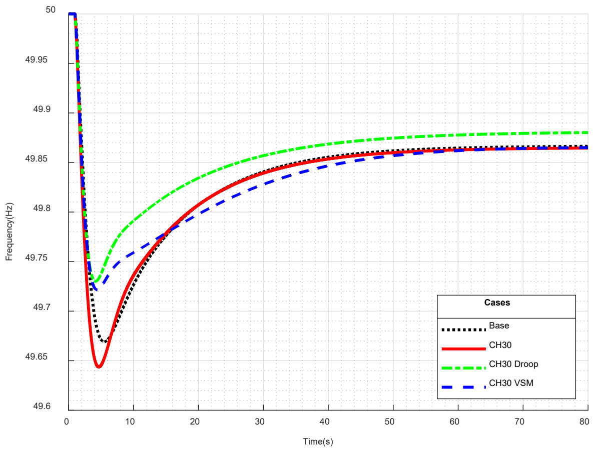

Fig. 6: Frequency comparison between the Base scenario, the CH2030 and the CH2030 GFM scenarios.

In Fig. 7 the output power of generators and converter are shown for the CH2030 GFM Scenario.

Here, unlike in the CH2030 scenario, the presence of RES generation is mitigated by using GFM devices. The SGs are aided by the presence of the GFM inverters, that participate in frequency stabilization by delivering active power during the transient. As shown in Fig.5, the inverter responses present some differences. The Droop GFM inverter’s response is characterized by a step-like response, with an initial overshoot, that helps the grid during the first seconds of the transient. Then it stabilizes at the steady state power related to its droop parameter. On the other hand, the VSM GFM inverter’s power response helps in the containment of the frequency deviation by providing power during the transient, however its contribution to the steady state frequency is null. This is because the VSM is similar to the droop control, with the addition of a low-pass filter in counter reaction. This control topology cancels the steady state droop contribution of the VSM.

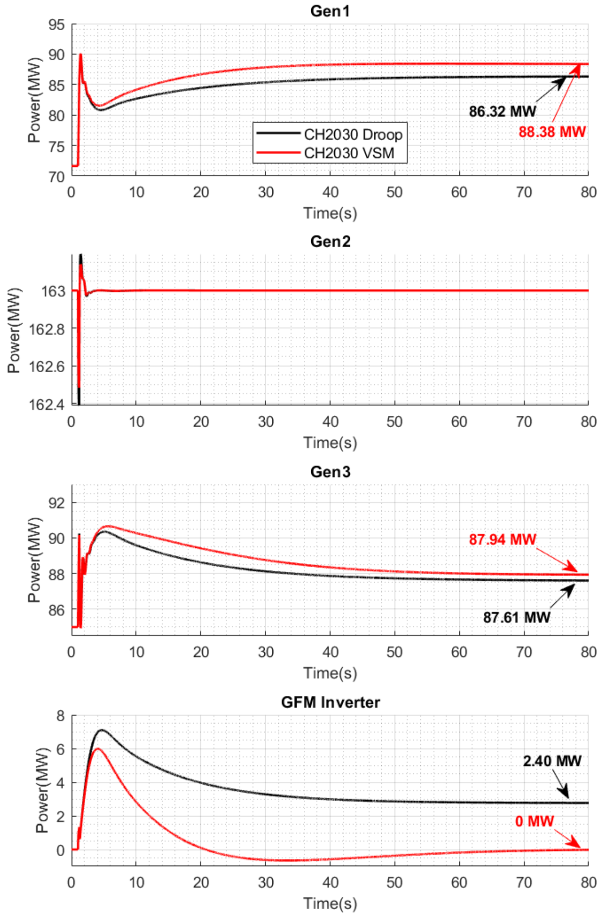

Fig. 7: Comparison of the active power responses between Droop and VSM for the CH2030 GFM Scenario

D. CH2040 Scenario

The expected Swiss generation mix for 2040 (Table I) is used to build this scenario. Here, the percentage of RES generation goes up to about the 56%, of which 53% is PV. To model this RES percentage in the IEEE9-bus system, Gen2 and Gen3 are substituted with two PV plants which, as previously, are implemented using the DER-A model. Consequently, Gen1 is the only SG in this scenario. The frequency and power results of the dynamic simulation are shown in Fig. 8 and 9.

As it can be expected, increasing the presence of GFL RES generation decreases the capacity of the system to mitigate the frequency transient. In this scenario, since only one SG provides support to the entire system, the frequency goes through a severe transient, during which a nadir of 49.482Hz is reached at $t = 5.55s$. Fig. 8 also shows that compared to the Base scenario, the RoCoF is higher and the steady state frequency is lower. Fig.6 b) shows how the active power responses of Gen1 covers the whole load unbalance due to the disturbance, while the two PV systems do not contribute to control frequency.

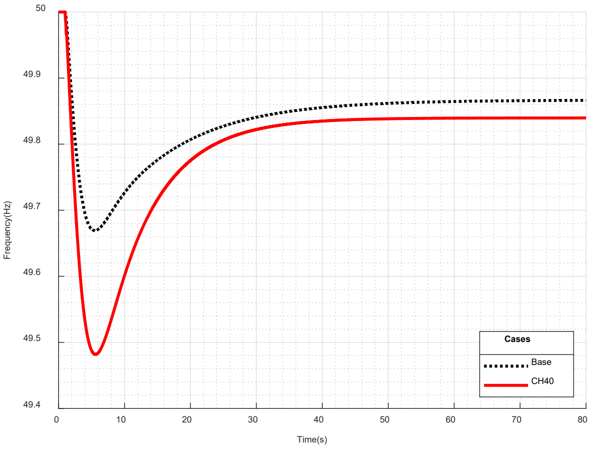

Fig. 8. Frequency response for the CH2040 scenario

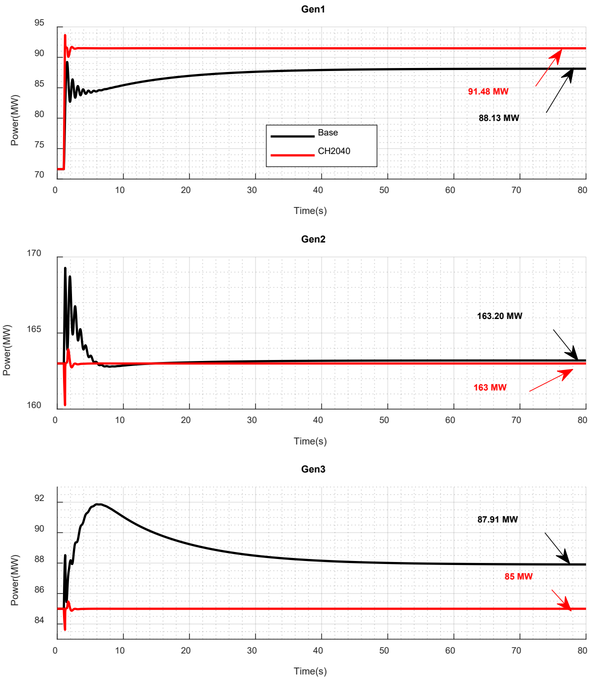

b)

Fig. 9. Active power response for the CH2040 scenario.

E. CH2040 GFM Scenario

As for the CH2030 GFM scenario, in the CH2040 GFM scenario a modeled 10 MVA GFM device is added to bus 8 to support the network. As previously, the two GFM models are used and compared and the same disturbance is applied. Fig. 10 shows the frequency response and Fig. 11 shows the active power response.

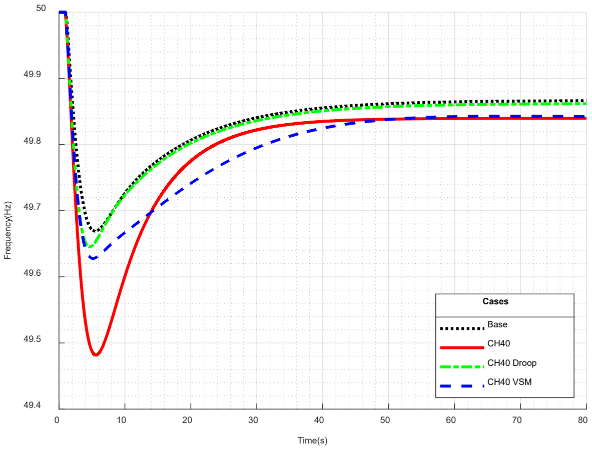

Fig. 10: Frequency comparison between the Base scenario, the CH2040 and the CH2040 GFM scenarios.

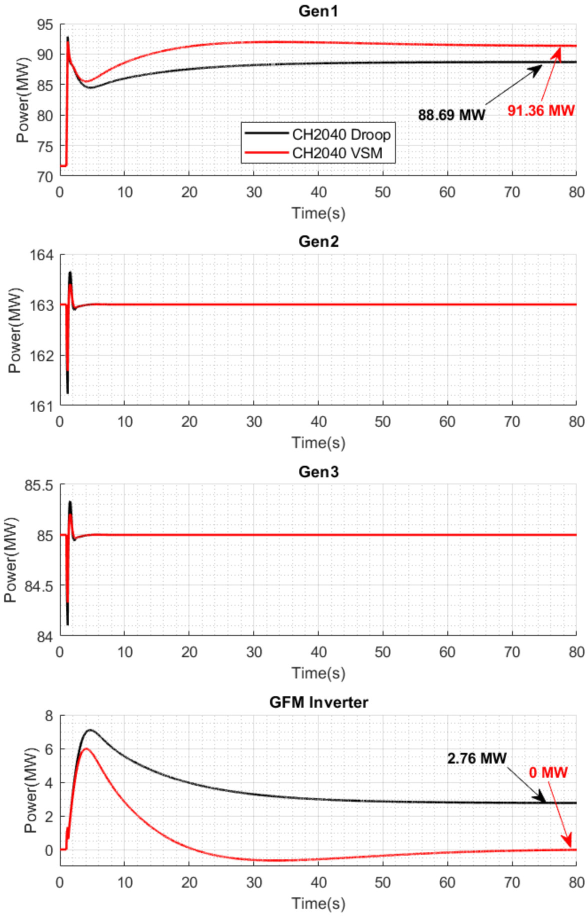

Fig. 11: Comparison of the active power responses between Droop and VSM for the CH2040 GFM Scenario

In Fig.7 the frequency behaviors obtained using GFM inverters are compared with the ones of the Base and CH2040 scenarios, this comparison shows the advantages introduced by these devices. The most evident is the enhanced value of frequency nadir, 49.645Hz at $t = 4.59s$ for the Droop control and 49.628Hz at $t = 5.11s$ for the VSM. Furthermore, the values of RoCoF are improved leading to slower initial deviations. This is due to the active power injection of the GFM devices in the initial period of the transient. Concerning the steady state values of the frequency, as previously, the Droop GFM effectively helps the system to stabilize the frequency faster and to a higher value with respect to the VSM controlled inverter. This is the consequence of the final output power of these inverters, that are about 3 MW and 0 MW for the Droop and VSM inverters respectively.

F. *Sensitivity analysis: Inverter size*

In order to assess how the GFM device's size impacts the frequency transient, notably the effect on frequency nadir, a sensitivity analysis has been carried out. This analysis is done considering the use of the Droop and VSM GFM inverters in the CH2030 scenario. For both the control algorithms, four sizes have been tested, starting at 2.5 MVA and doubling up to 20 MVA. The results obtained from the analysis regarding frequency and active power are summarized in Table II and III. The percentages values used represent the percentage of GFM MVA with respect to the synchronous generation present in the system.

TABLE II
FREQUENCY NADIR AND TIME VALUES

	DROOP				**VSM**			
UNIT SIZE (MVA)	2.5 (0.7%)	5 (1.3%)	10 (2.7%)	20 (5.3%)	2.5 (0.7%)	5 (1.3%)	10 (2.7%)	20 (5.3%)
TIME (S)	4.485	4.360	4.095	3.680	4.565	4.475	4.310	4.060
NADIR (Hz)	49.672	49.694	49.730	49.782	49.668	49.688	49.722	49.772

TABLE III
MAX POWER AND TIME VALUES

	DROOP				**VSM**			
UNIT SIZE (MVA)	2.5 (0.7%)	5 (1.3%)	10 (2.7%)	20 (5.3%)	2.5 (0.7%)	5 (1.3%)	10 (2.7%)	20 (5.3%)
TIME (S)	4.550	4.410	4.160	3.785	3.905	3.830	3.680	3.415
POWER (MW)	1.642	3.063	5.397	8.711	1.363	2.574	4.630	7.703

As can be seen, as the size of the inverter increases, the frequency nadir value increases while the time at which it occurs decreases. This is because larger units deliver more power in a shorter time.

G. *Sensitivity analysis: Network Loading*

A further sensitivity analysis has been done on the network loading. To do this, the dynamic analysis is run applying the same 20% load variation at Load8, as done before, but the initial power dispatched by the generators is redistributed according to their size. Starting from the load values used previously (Load5=125MW, Load6=90MW and Load8=100MW), the total load is increased until the load leads to an instable transient. The load limits are summarized in Table IV, in which they are expressed as a percentage of the base load. These results show that for the CH2030 and the CH2040 scenarios, without the help of GFM inverters, the network loading applicable to the grid decreases, demonstrating a weakening of the grid. The use of GFM inverters, allows this limit to increase, making the network stronger.

TABLE IV
MAX NETWORK LOADING

	Base	CH2030	CH2040
Without GFM	152%	151%	139%
GFM Droop	-	153%	141%
GFM VSM	-	151%	149%

V. CONCLUSION

As expected, replacing synchronous generation units with RES generation units causes a weakening of the system leading to potential stability problems. This work focused on frequency stability issues caused by a rapid load increase and demonstrated how they can be resolved by supporting the grid with GFM inverters able to provide services such as synthetic inertia. These devices have the advantage of having the ability to provide support even in weak and low inertia grids. Indeed, although preliminary, the results show a clear improvement in the frequency profiles when a GFM inverter is used to support the system. Depending on the requirements, the effectiveness of the GFM inverter can be emphasized on its ability to provide synthetic inertia, to mitigate abrupt frequency transient in the first moments after the disturbance, or on active power to favor the containment of the frequency deviation. This highlights the need for further development of GFM converters and the coordination of new grid services and market products to encourage their use and promote RES integration to achieve energy transition goals.

REFERENCES

[1] Scenario framework 2030/2040 for electricity network planning, Swiss Federal Office of Energy.

[2] Grid-Forming Technology in Energy Systems Integration, Report by the Energy Systems Integration Group's High Share of Inverter-Based Generation Task Force, March 2022

[3] UNRUH, Peter, et al. Overview on grid-forming inverter control methods. Energies, 2020, 13.10: 2589.

[4] LIN, Yashen, ETO, Joseph H., JOHNSON, Brian B., et al. Pathways to the next-generation power system with inverter-based resources: Challenges and recommendations. IEEE Electrification Magazine, 2022, vol. 10, no 1, p. 10-21.

[5] BADESA, Luis, MATAMALA, Carlos, ZHOU, Yujing, et al. Assigning Shadow Prices to Synthetic Inertia and Frequency Response Reserves from Renewable Energy Sources. IEEE Transactions on Sustainable Energy, 2022, vol. 14, no 1, p. 12-26.

[6] D'ARCO, Salvatore; SUUL, Jon Are. Equivalence of virtual synchronous machines and frequency-droops for converter-based microgrids. IEEE Transactions on Smart Grid, 2013, 5.1: 394-395.

[7] Nine-bus System, DIgSILENT PowerFactory.

[8] POURBEIK, P., et al. An aggregate dynamic model or distributed energy resources or power system stability studies. Cigre Science & Engineering,(14), 2019, 38-48.